

# ASSOCIATION BETWEEN REDUCTION IN CEREBRAL BLOOD FLOW AND AXONAL TRANSPORT DEFICITS IN MOUSE MODELS OF DIABETES USING MRI.

F. Serrano<sup>1</sup>, T. Terashima<sup>2</sup>, S. K. Amin<sup>3</sup>, L. Hu<sup>1</sup>, L. Chan<sup>2</sup>, and R. Pautler<sup>1,4</sup>

<sup>1</sup>Molecular Physiology and Biophysics, Baylor College of Medicine, Houston, TX, United States, <sup>2</sup>Medicine, Baylor College of Medicine, Houston, TX, United States, <sup>3</sup>Molecular Physiology and Biophysics, Baylor College of Medicine, Houston, TX, <sup>4</sup>Neuroscience, Baylor College of Medicine, Houston, TX, United States

**Introduction:** Diabetes mellitus is a multifactorial disease characterized by high levels of serum glucose (hyperglycemia) as a result of insulin deficiency, attenuation of insulin action or a combination of both [1]. Hyperglycemia is associated with several complications primarily vascular disease affecting small (microvascular) or large (macrovascular) vessels individually or in combination. Studies on humans and experimental models of diabetes have shown that acute and chronic hyperglycemia causes decreases in cerebral blood flow; however, the mechanism is not yet completely understood [2, 3]. One possible consequence of microvascular disease is the development of neuronal dysfunction ultimately resulting in diabetic neuropathy. However, additional factors could also be involved in the pathogenesis of neuropathy including direct effects of hyperglycemia on neurons and intracellular metabolic changes that impair nerve function.

A common experimental animal model of diabetes is produced by the injection of the drug streptozotocin (STZ). STZ causes a selective destruction of pancreatic beta cells leading to hypoinsulinemia and chronic hyperglycemia. Using Manganese-Enhanced MRI (MEMRI) we have been able to observe axonal transport deficits in the olfactory bulb as early as 1 wk after STZ injection [4]. Thus, the goal of our study is to use two imaging modalities (Arterial Spin labeling and MEMRI) to investigate the association between cerebral blood flow (CBF) dysfunction and axonal transport deficits. Evaluating both CBF and axonal transport deficits *in vivo* using MRI will be useful in the investigation of the underlying mechanisms of hyperglycemia induced CBF perturbations and neuronal dysfunction in animal models.

**Methods: Diabetes models: Chronic hyperglycemia:** C57BL/6 (23-25g) mice were injected intraperitoneally (IP) with 170mg/kg streptozotocin (STZ) made in sodium citrate buffer pH4.5. Body weight and glucose levels were checked before and after STZ-injections. Mice are considered diabetic if glucose levels were higher than 200mg/dl. In this study we examined mice 2 wks after were injected: with saline (n= 3); STZ (n=3); and STZ and an insulin pellet (n= 4). **Acute hyperglycemia:** C57BL/6 (23-25g) mice were injected intraperitoneally (IP) with a 25% solution of D-glucose. This treatment causes an increase in serum glucose levels that peak after 15 min and last for about 2 hrs at which time levels go back to normal serum glucose levels.

**Manganese Enhanced MRI (MEMRI):** Axonal transport analysis was performed using MEMRI in the olfactory bulb. Mice were anesthetized using 5% isoflurane in 100% oxygen. Following anesthesia, 4 $\mu$ l (2 $\mu$ l/naris) of a 0.77g/ml solution of MnCl<sub>2</sub> was pipetted into the nasal cavity of each mouse. Mice were allowed to recover for 45 min in a warming pad which also facilitated the uptake of Mn<sup>2+</sup> into the olfactory receptor neurons in the olfactory epithelium. Mice were placed in a horizontal bore 9.4T Bruker Advanced imaging system and maintained in 1-2% isoflurane for the remainder of the imaging session. The imaging parameters were as follows: multi-slice/multi echo 2D imaging protocol; matrix dimensions = 128 x 128; FOV: 3.0cm x 3.0cm; slice thickness = 1mm; repetition time (TR) = 500ms; echo time (TE) = 10.2 ms; NA = 2; and number of repetitions = 15 for a total image time of 32 min. First scan was started 60 min after Mn<sup>2+</sup> lavage (zero time point). Four axial slices (1 mm thickness; 1mm interslice thickness) were selected with the 1<sup>st</sup> slice aligned within the edge of the olfactory bulb (slice #4, sagittal slice). The actual pixel which corresponded to the ROI was localized about 50% of the length along the lateral portion of olfactory bulb. Changes in the pixel intensity were measured using Paravision software (v 3.02) and the changes in slope were compared among groups. Values were plotted as changes in signal intensity over time ( $\Delta SI/t$ , as percent of controls) and statistical analysis were done using Prism. All signal intensities were normalized to non-enhanced muscle outside the brain.

**Perfusion Arterial Spin Labeling (ASL):** The imaging parameters were as follows: TR = 7145.973 ms, TE = 24.26 ms, Number of averages = 1. The inversion recovery time (TIR) = 100ms, the number of TIR = 8, the TIR increment = 1000 ms, the inversion slab thickness = 6 mm, and the slice package margin = 2.50 mm. The effective bandwidth = 200kHz. The field of view (FOV) = 15 x 15 mm, matrix = 64 x 64 and slice thickness = 1mm. We utilized Bruker Biospin's Paravision 4.0 software to calculate the rCBF. Briefly, the imaging slice was positioned transversely through the olfactory bulb (OB) for both the slice selective and non-selective slice T1 series. Regions of interests (ROI) were defined for the calculation of the T1 images for both the T1 series: right OB, left OB. The data points from each ROI were fitted to a T1 inversion regression curve. The values are used to calculate CBF according to: Relative CBF (rCBF) =  $\lambda (1/T1_{selective} - 1/T1_{nonselective})$  where  $\lambda$  is the blood-brain partition coefficient, which was set to 90ml blood/100g of tissue. The factor 60000 was used to convert milliseconds to minutes and, consequently, the unit for rCBF is ml/(100g\*min). The rCBFs were compared among groups and graphed using the graphing, Prism.

**Results:** In our chronic model of hyperglycemia we observed deficits in axonal transport in the olfactory bulb 2 weeks after the injection of STZ as compare to control mice (Fig. 1). Furthermore, mice treated with an insulin pellet (STZ + Ins) showed a significant improvement in axonal transport. No statistical differences were observed between the control and STZ + Ins groups (Fig. 1). We also have performed preliminary studies on rCBF levels in the same groups of mice and observed that mice treated with STZ have decreased cerebral blood flow in the olfactory bulb (Fig.2). Furthermore, mice treated with insulin appear to have improved rCBF. We have also investigated if acute hyperglycemia causes deficits in axonal transport and observed no change in axonal transport after a single injection of glucose (data not shown).

**Conclusions and Future Directions:** Several mechanisms are thought to contribute to the pathogenesis of diabetic neuropathy including alterations in blood flow and neuronal function; however, it is not clear if these events occur consecutively or coincidentally. Our current data suggest that there is an association between attenuation in CBF and deficits in axonal transport during chronic hyperglycemia. This is consistent with the association between blood flow and neuronal activity that is the basis of fMRI. We did not observe deficits in axonal transport during acute hyperglycemia thus we will investigate if insulin treatment causes reductions in rCBF. A reduction in rCBF would suggest that axonal transport deficits are consequential to alterations in CBF and that chronic hyperglycemia is necessary for the vascular dysfunction to impact neuronal function. The possibility to evaluate the impact of hyperglycemia on microvascular dysfunction and neuronal physiology *in vivo* using MRI in animal models of diabetes may provide a useful system to understand the mechanism of hyperglycemia induced neuropathy.

**References:** 1. American Diabetes Association, Diabetes Care, 2006. 29 p. S43-8. 2. Novak, V., et al., Diabetes Care, 2006. 29(7): p. 1529-34. 3. R. B. Duckrow, et al., Stroke, 1987. 18: p. 52 - 58. 4. F. Serrano, ISMRM poster, 2006.

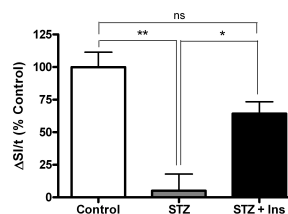


**Fig 1. Insulin reverses axonal transport deficits in STZ mice**

Graph shows axonal transport as determined by changes in signal intensity over time ( $\Delta SI/t$ ). Control mice (n=3), STZ-treated mice (n=3), and STZ + Ins (n=4). \* p < 0.05; \*\* p < 0.001, ns (not significant).

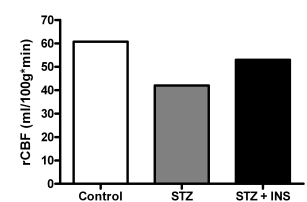


**Fig 2. Insulin reverses rCBF deficits in STZ mice**

Inverse regression curves using ASL showing changes in rCBF. Control (n=2), STZ (n=2), STZ + Ins (n=1).